9th European Workshop on Structural Health Monitoring
July 10-13, 2018, Manchester, United Kingdom

Coda Wave Interferometry used to detect loads and cracks in a concrete structure under field conditions

Xin WANG[1], Ernst NIEDERLEITHINGER[2]
1 BAM, Germany, xin.wang@bam.de
2 BAM, Germany, ernst.niederleithinger@bam.de

Abstract

Nowadays, the excessive use and environmental factors have accelerated the deterioration of concrete bridges. Coda Wave Interferometry (CWI) for ultrasonic data is one of the most promising methods to detect subtle changes in heterogeneous materials like concrete. The advantage of this method is that large volume structure can be monitored by a limited number of sensors using multiply scattered waves. However, previous research results objects on cracks detection and localization using the CWI method are mostly limited to laboratory size concrete. Till now, it is still difficult to separate and quantify the influence factors such as cracks, stress and temperature especially under outdoor environment. To evaluate the various influence factors, data integration with other types of sensors and the improvement of CWI method are necessary. In this paper, detection of loads and cracks in a 24.4 meters long pre-tensioned reinforcement concrete beam with multiple sensors installed including a new type of embedded ultrasonic sensor and which was situated under field environment will be examined by integrating CWI technics with others. As a result, cracks should be identified in a rough range or even more precise.

1. Introduction

Traditionally, structure health monitoring and modal analysis by sonic or vibration measurements are done in a frequency range below 20 kHz (1). However, the wavelength is larger than the macroscopic size of the structure and the sensitivity to microscopic features is limited (2). To reach a higher precision and sensitivity, a method from seismology called Coda Wave Interferometry has been used in several studies (3). The working frequency of this method is higher than 50 kHz so that the waves enter multiply scattering regime and interact with the heterogeneities (1). Coda wave interferometry has been shown to be very sensitive to subtle changes in the structure. CWI was applied to monitor water saturation in sandstone (4), stress related velocity change (5) and thermally induced velocity change (6). It was also used to detect and locate cracks in concrete (7). However, these experiments have been carried out on limited size concrete specimen in laboratories. Only a few trials were performed under outdoor environmental conditions (8).
To assess the performance of the CWI method under more realistic conditions, several embedded ultrasonic sensors SO807 (9) have been installed inside a new reference structure at an outdoor experimentation facility, which was then subjected to various load conditions.

2. Coda wave interferometry

As diffuse waves travel along much longer paths than direct or simply reflected ones, they are much more sensitive to weak perturbation of the medium. The principle of CWI is to compare the coda waves recorded in two different states to monitor weak velocity variations as well as some other parameters. As shown in Figure 1, two signals are recorded before and after perturbation. The first arrivals of the signals are almost the same, while the coda wave (later arrivals) shows a significant difference.

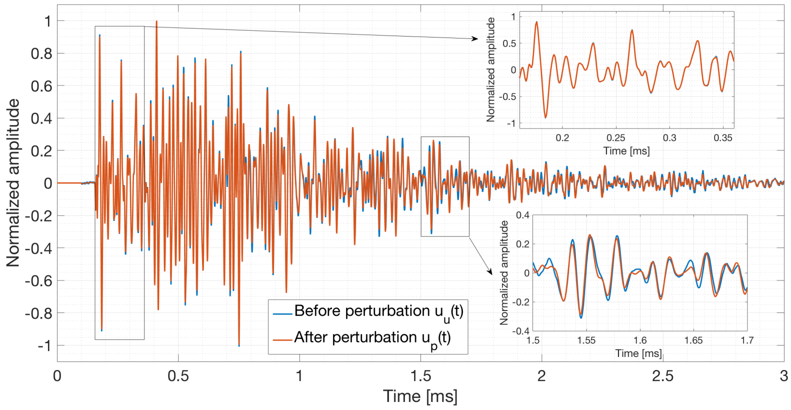

Figure 1. Signal recorded before perturbation ($u_u(t)$) and after perturbation ($u_P(t)$)

The most used method to evaluate these changes is the stretching method (10) where the velocity change is considered as a dilation or compression in time by a factor α (Eq. (1)).

$$u_P(t) = u_u(t(1+\alpha)) \tag{1}$$

A reference signal must be selected firstly. Typically, the signals recorded before the perturbation are determined as the reference signals. As the last part of the signal is noise basically, a suitable window must be chosen and applied to the reference signal. Then the reference signal will be stretched by different factors α in a range [-dv, dv] with a resolution of 0.01% or even 0.001%, depending on different situations. Then the cross-correlation between the signal recorded after the perturbation and all the stretched signals which measure the similarity of these signals will be calculated by Eq. (2). The best α which maximizes the cross-correlation will be chosen as the relative velocity change (dV/V).

$$CC(\alpha) = \frac{\int_{t-T}^{t+T} u_u(t'(1+\alpha))u_p(t')dt'}{\sqrt{\int_{t-T}^{t+T} {u_u}^2(t')dt' \int_{t-T}^{t+T} {u_p}^2(t')dt'}} \tag{2}$$

3. The reference structure and experimental setup

3.1 BLEIB reference structure

The BLEIB reference structure (Fig.1) was designed and built for different groups from different departments of BAM to analyse load influence with different techniques. The structure is a 24.4-meter-long inverse u-shaped post-tensioned (600 kN load on each of two tendons) reinforced concrete beam with multiple sensors installed, such as ultrasonic transducers, optical fibers, accelerators, etc. Two loads of two tons each were used for the static test and a shaker of 30.6 kg was used for the dynamic test. The BLEIB reference structure is as well used as a shared object for the EU project INFRASTAR.

Figure 2. BLEIB reference structure at the BAM test site

14 embedded ultrasonic transducers of type ACS SO807 (8) sensors were installed inside the structure distributed in 5 cross-sections (A, B, C, D, E). Embedded transducers were used as they ensure constant coupling, and less influence from surface waves and near surface changes (e.g. temperature influence). The positions of these transducers are shown in Fig.3 marked with different colours. Transducers No.1 ~ No.8 were situated around the centre of the left part of BLEIB structure while transducers No.11 ~ No.14 were in the right part. Transducers No.9 and No.10 were installed in the middle of the beam, which were also above the middle bearing.

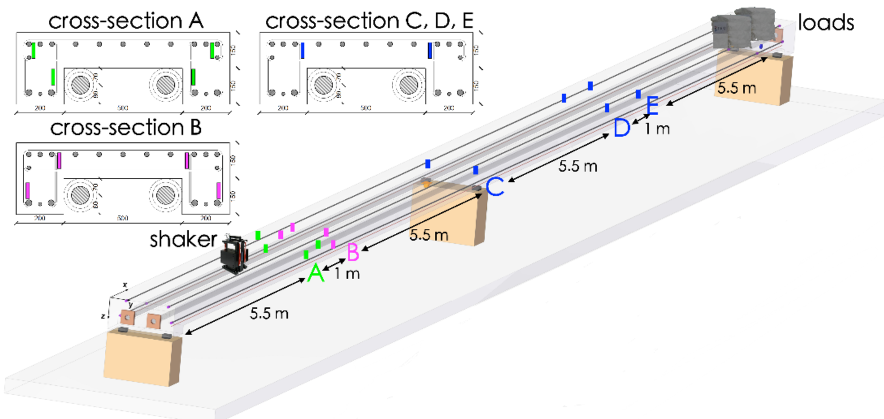

Figure 3. Positions of ultrasonic sensors in BLEIB reference structure

To provoke certain limited damage in one of the spans, the tension was released and the loads were moved from the end of the beam to the middle of one span to create some cracks spread from the bottom. Most of the cracks appeared around cross-section D and E where sensor No.11 ~ No.14 were located (Fig.4). Then the tension was reloaded again, and all the cracks closed.

Figure 4. Positions of the cracks marked with maker pen

3.2 Dynamic test and static test

3.2.1 Dynamic test

A shaker with a frequency range of 0 – 100 Hz and weight of 30. 6 kg was placed 4.2 meters away from the left edge of the BLEIB structure (Fig. 3). During the test, the shaker ran in a random frequency mode with an upper frequency of 60 Hz and a lower frequency of 2,6 Hz for 15 minutes. One load was positioned on the middle bearing, and the other load was positioned at the far end of BLEIB structure.

3.2.2 Static test

The two loads moved step by step from the right extremity of BLEIB structure to the left extremity. Time and position information of the loads are shown in Fig.5. The static test lasts about one hour. The ultrasonic transducers kept measuring all along the test.

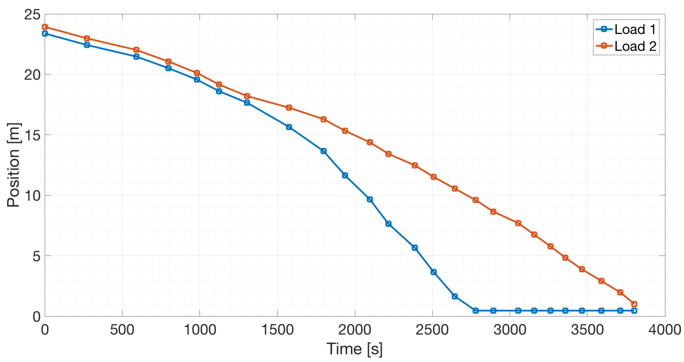

Figure 5. Positions of loads in each step

4. Result

4.1 Dynamic test

As the shaker is only 30.6 kg, the impact is weak comparing to the 2-tons-load. As the expected changes in the structure are small, high sensitivity and precision are required. While calculating the velocity change, a resolution of 10^{-3} % (5) and a time window of [0, 3ms] are selected. The full signal length is 5 ms.

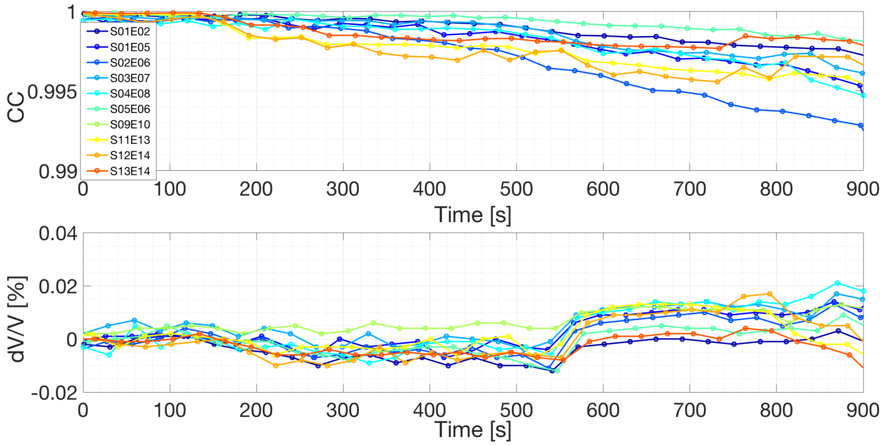

Figure 6. Correlation coefficient and velocity change of dynamic test

The displacement and deformation of BLEIB structure increased over time according to experience and the correlation coefficient (CC) decreased. The velocity change (dV/V) of combination S09E10 (transmitter 09 and receiver 10), which is in the middle of the beam and under the load are always positive. The dV/V of all other combinations started to increase with the same trend (Fig 6) from 540 seconds. During the whole dynamic test, the CC varied in range [0.9929, 1] and the dV/V varied between range [-0.012 %, 0.021%] which shows the sensitivity of CWI method.

4.2 Static test

The digital image correlation system measured the displacement of BLEIB structure during the static test. The 7th load step is the step in which the structure has the biggest displacement (Fig 7). Cross-section D and E moved about 37 mm down, meanwhile cross-section A and B moved about 15 mm up, while the displacement of cross-section C is negligible. The displacement of 5 points close to these five cross-sections in each load step are shown in Fig 7.

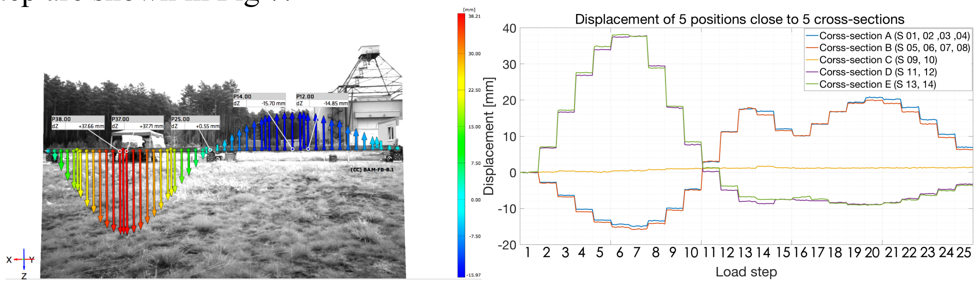

Figure 7. Biggest displacement (left) and displacements of 5 cross-sections in each load step

The influence of loads led to a much bigger velocity change. To speed up the calculation, the resolution could be appropriately reduced. In this case, a resolution of 10^{-2} % and a signal window [0, 3 ms] are selected.

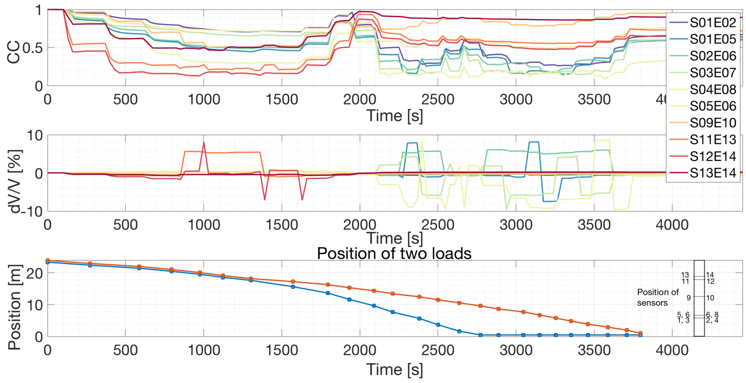

Figure 8. Correlation coefficient and velocity change of static test of all combinations

The different load steps could be identified according to the CC and dV/V (Fig. 8, 9). The CC of the combinations far from the loads changed less, while those of the combinations near the loads changed more. For load step 11 (both load above the centre bearing) the values return almost back to 1. As shown in Fig. 7, the displacement of cross-section A, B, C and D started to change sign between load step 10 and 11 so did the velocity changes (Fig. 8, 9 around 1960 seconds). The curve shapes of velocity change of combinations in cross-section A and B correspond well to the displacement of cross-section A and B before the before step 11 as the loads are far away from these cross-section, on the other hand, the curve shapes of velocity change of combinations in cross-section C and D correspond well to the curve shapes of the displacement of cross-section C and D for the same reason. (Fig. 9)

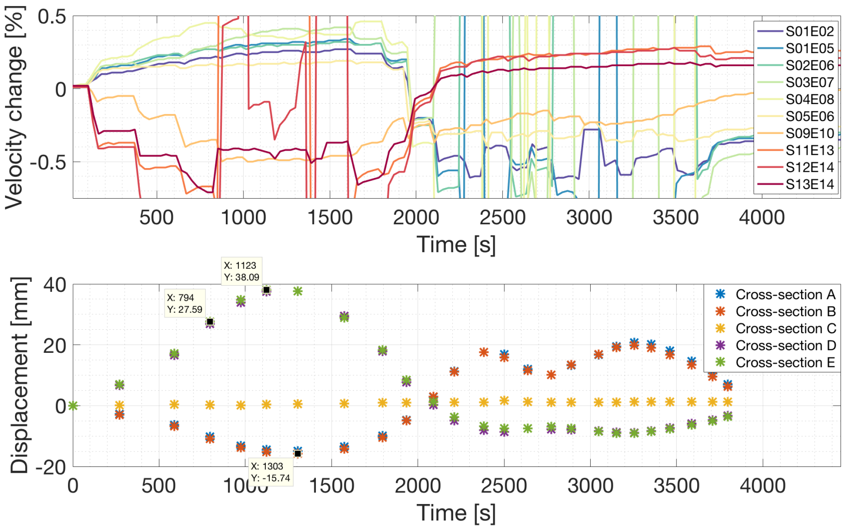

Figure 9. Top: velocity change of static test of all combinations, velocity change limits are set to [-0.75, 0.5] mm, bottom: displacement of 5 cross-sections in 25 steps

However, for some combinations of sensors (S01E05, S02E06, S11E13, S12E14, etc.) which were installed in different cross-sections and parallel to the structure, the velocity changed suddenly from less than 1% to more than 5% (Fig. 8, 9), which means the changes in the structure are too big. Between load step 4 and 7, the displacement of cross-section D and E increased from 27.59 mm to 38.09mm (Fig. 9) which leaded to the cracks opening and the waves which were supposed to pass through this area were strongly disrupted. The dV/V of S11E13 and S12E14 which are closed to the cracks started to increase which is an unusual behaviour, either the chosen window or the CWI method is not applicable anymore. These signals need to be analysed. After load step 11, the displacement of cross-section D and E increased from 0 to 9 mm upwards, the CC and dV/V of combination S11E13, S12E13 and S13E14 changed slowly and remained quite stable as these transducers are far away from the loads and all the cracks between cross-section D and E were closed. No new cracks spread from the top of the structure were created.

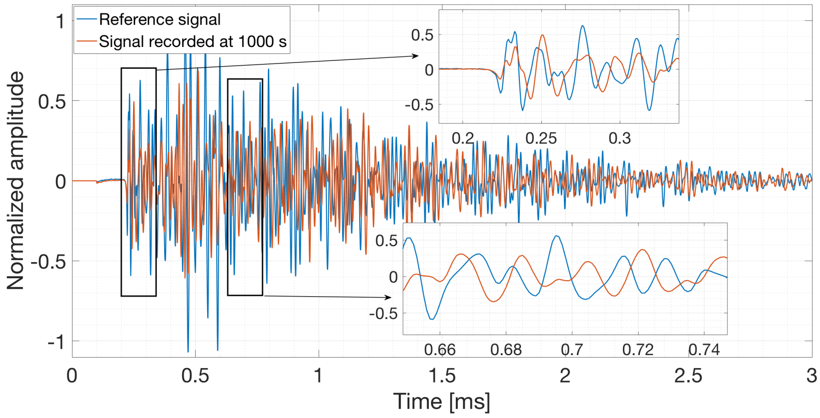

Figure 10. Velocity change of static test of all combinations

The signal recorded at 1000 seconds which is in the unusual velocity change behaviour area of S11E13 changed totally comparing to the reference signal (Fig. 10). It is impossible to identify weather the wave is dilated or compressed by coda wave because the time phase shift was too big (e.g. Fig. 10 [0.66ms, 0.74ms]). Even the first arrivals had a noticeable change in amplitude and time phase. This is against the CWI theory. The changes in the structure were not subtle any more. Macro cracks must have been created. The dV/V of combination S13E14 which the sensors were installed in the same cross-section varied around 0.4 % (Fig. 9) which is reasonable in this unusual behaviour area of S11E13 so that these macro cracks must be in the area between the cross-section D and E.

4. Conclusions

In this experiment, the dynamic test showed that CWI method has a high sensitivity (10^{-3} %) in wave propagation velocity change. When the change in the structure is weak, a higher precision must be chosen. The static test showed that CWI method is sensitive to load effect. When the loads pass through an area, before the cracks appear, the bending tensile stress increased and the velocity change decreased, on the contrary, in the area where is on the opposite side of the structure, the compression stress increased and velocity change increased (11). With the move of the loads, the level of the velocity change and displacement had the same trend. When the change in the structure is big enough, a low resolution will accelerate the calculation and the result can be still precise. However, when macro cracks appear due to the move of loads, the signals change too much comparing to the reference signal. Consequently, either a smaller window need to be chosen or the CWI method is not applicable anymore depends on the cracks width. As a next step, data integration with optical fiber sensors, which can identify cracks and quantify their width, will be studied.

Acknowledgements

This research is supported by INFRASTAR project which has received funding from the European Union's Horizon 2020 research and innovation programme under the Marie Skłodowska-Curie grant agreement No 676139.
Thanks to Mr Klaus-Peter Gründer from BAM division 8.1 for providing me the DIC data and results. Thanks to my office college Ms Anja-Sophie Bertschat, who works on CWI, for the help.

References

1. T Planès, E Larose, "A review of ultrasonic Coda Wave Interferometry in concrete." Cement and Concrete Research 53, pp 248-255, 2013.
2. JA Bogas, MG Gomes, A Gomes, "Compressive strength evaluation of structural lightweight concrete by non-destructive ultrasonic pulse velocity method", Ultrasonics, 53(5), pp 962-972, 2013.
3. A Grêt, "Time-lapse monitoring with coda wave interferometry", Diss. Colorado School of Mines, 2004.
4. A Grêt, R Snieder, JScales, "Time-lapse monitoring of rock properties with coda wave interferometry", Journal of Geophysical Research: Solid Earth 111.B3, 2006.
5. E Larose, H Stephen, "Monitoring stress related velocity variation in concrete with a 2× 10− 5 relative resolution using diffuse ultrasound", The Journal of the Acoustical Society of America 125.4 pp 1853-1856, 2009.
6. E Niederleithinger, C Wunderlich, "Influence of small temperature variations on the ultrasonic velocity in concrete", In AIP Conference Proceedings, Vol. 1511, No. 1, pp. 390-397, 2013.
7. E Larose, A Obermann, A Digulescu, T Planes, JF Chaix, F Mazerolle,G Moreau, "Locating and characterizing a crack in concrete with diffuse ultrasound: A four-point bending test", The Journal of the Acoustical Society of America, 138(1), pp 232-241, 2015.
8. SC Stähler, C Sens-Schönfelder, E Niederleithinger, "Monitoring stress changes in a concrete bridge with coda wave interferometry", The Journal of the Acoustical Society of America, 129(4), pp 1945-1952, 2011.
9. E Niederleithinger, J Wolf, F, Mielentz, H Wiggenhauser, S Pirskawetz, "Embedded ultrasonic transducers for active and passive concrete monitoring". Sensors, 15(5), pp 9756-9772, 2015.
10. C Sens-Schönfelder U Wegler, "Passive image interferometry and seasonal variations of seismic velocities at Merapi Volcano, Indonesia", Geophysical research letters, 33(21), 2006.
11. E Niederleithinger, M Herbrand, M Müller, "Monitoring von Querkraftversuchen an Spannbetondurchlauf trägern mit Ultraschall und Codawelleninterferometrie", Frequenz, 20(70), pp 50-60, 2017.